Efficient method for the quantum Monte Carlo evaluation of the static density response function of a many-electron system

R. Gaudoin[1,*] and J. M. Pitarke[2,3]

[1]*Donostia International Physics Center (DIPC), Manuel de Lardizabal Pasealekua, Donostia, E-20018 Basque Country, Spain*

[2]*CIC nanoGUNE Consolider, Tolosa Hiribidea 76, Donostia, E-20018 Basque Country, Spain*

[3]*Materia Kondentsatuaren Fisika Saila (UPV/EHU) and Centro Física Materiales (CSIC-UPV/EHU), 644 Posta kutxatila, E-48080 Bilbo, Basque Country, Spain*

(Received 19 October 2009; revised manuscript received 5 February 2010; published 17 June 2010)

In a recent letter we introduced Hellmann-Feynman operator sampling in diffusion Monte Carlo calculations. Here we derive, by evaluating the second derivative of the total energy, an efficient method for the calculation of the static density-response function of a many-electron system. Our analysis of the effect of the nodes suggests that correlation is described correctly and we find that nodal issues can be dealt with.

DOI: 10.1103/PhysRevB.81.245116 PACS number(s): 71.10.Ca, 71.15.−m

I. INTRODUCTION

Diffusion Monte Carlo (DMC) represents a powerful method for the accurate computation of properties of molecules and solids.[1] However, so far few attempts[2,3] have been made to use DMC to calculate the static density-response function,[4] which is a central quantity in the analysis of many-electron systems and time-dependent density-functional theory.[5] One reason is the technical difficulty inherent in the most straightforward method to do so: for a given perturbing potential one calculates the total energy at different strengths and numerically determines the second derivative. This then gives a DMC estimate of the diagonal term of the static response function χ. There are, however, several obvious difficulties with this. One needs one loop for various perturbation strengths, another loop for each k that one wishes to sample, and if one wants the off-diagonal terms a third loop for the k'. Inside each of these loops sits an entire wave function reoptimization cycle and a complete DMC run. The perturbations must be small enough not to change the wave function qualitatively and large enough to allow for sensible numerical derivatives.

In a recent letter,[6] we showed how "applying" the Hellmann-Feynman[7] (HF) derivative to the DMC algorithm leads to a new algorithm, Hellmann-Feynman sampling (HFS), that correctly samples the first derivative of the energy, i.e., an expectation value of an operator. HFS works because DMC yields the correct total energy for nodes defined by the trial wave function. For technical reasons the operators sampled must be diagonal in real space. Extending the analysis to the second derivative yields a DMC algorithm for the frozen-node (fn) static density-response function. Note that even for a trial wave function with correct nodes the frozen-node density response is not exact as the real response includes effects from the change of the nodes, hence the moniker frozen node. However, comparison with Ref. 2 where the nodal variation in an underlying Kohn-Sham (KS) system is implicitly used, shows that these effect can be accounted for by generalizing the RPA analysis[8] to fn systems. The resulting method can be performed within a single DMC run and in the case of inhomogeneous systems can produce off-diagonal elements of χ as easily as the diagonal terms.

The present paper is organized as follows. After a brief recapitulation of HF sampling, we derive formulas for the DMC sampling of χ along the same line. We then briefly discuss technical aspects (convergence with respect to population size, time step, etc.). Finally, we look at the density response of the interacting and noninteracting uniform electron gas, analyze the effects of the nodes, and compare our results with the literature. Our method should also enable DMC calculations of the static-response function of real solids, never done before. We use atomic units throughout.

II. HELLMANN-FEYNMAN SAMPLING AND THE DENSITY RESPONSE FUNCTION

A. Application to the second derivative of the energy

Fixed-node DMC yields by construction the normalized expectation value $\langle\hat{O}\rangle_{\mathrm{DMC}}=\langle\Psi_T|\hat{O}|\Psi_0^{\mathrm{fn}}\rangle/\langle\Psi_T|\Psi_0^{\mathrm{fn}}\rangle$, where Ψ_0^{fn} is the ground-state wave function constrained by the nodes of the Fermionic many-body trial wave function Ψ_T; HFS correctly calculates $\langle\Psi_0^{\mathrm{fn}}|\hat{O}|\Psi_0^{\mathrm{fn}}\rangle/\langle\Psi_0^{\mathrm{fn}}|\Psi_0^{\mathrm{fn}}\rangle$ while maintaining the basic DMC algorithm that samples $\Psi_T\Psi_0^{\mathrm{fn}}$. This is because the total energy is evaluated correctly within standard DMC and crucially operator expectation values can be cast as HF derivatives of the total energy. Keeping in mind that ultimately the DMC algorithm is nothing but a large sum that yields the total energy, we see that the HF derivative can be applied to the algorithm itself. One advantage over numerical derivatives is that the resulting formula can handle several operators simultaneously in a single DMC run and maintaining orbital occupancy for perturbed Hamiltonians ceases to be a problem. The DMC algorithm only involves numbers so noncommutability of operators is no problem. Writing down the DMC algorithm as a mathematical formula and applying the HF derivative to it yields an object that when sampled using standard DMC produces the *exact* operator expectation value. We find that given a Hamiltonian $\hat{H}(\alpha)=\hat{H}+\alpha\hat{O}$, evaluating the growth estimator of the energy E^{GR} at time step i to first order in α yields a growth estimator that samples the operator $\hat{O}$. Similarly the direct estimator E of the energy yields another estimator. These are Eqs. (8) and (9) of Ref. 6

$$O_i^{GR} = \left.\frac{\partial E_i^{GR}(\alpha)}{\partial \alpha}\right|_{\alpha=0} = \overline{X_i}, \tag{1}$$

$$O_i^{E} = \left.\frac{\partial E_i(\alpha)}{\partial \alpha}\right|_{\alpha=0} = \overline{O_i^L} - t(\overline{E_i^L X_i} - \overline{E_i^L}\cdot\overline{X_i}), \tag{2}$$

where the bar refers to the DMC sampling at time step i: $\overline{X_i}=\Sigma_j^{N_w}\omega_{i,j}X_{i,j}$. N_w is the possibly i dependent number of walkers, $\omega_{i,j}$ is the total weight of walker j, $X_{i,j}=\frac{1}{i}\Sigma_{k=1}^{i}O_{k,j}^L$, $t=i\Delta t$ the time of sampling, and $O_{k,j}^L$ is $\frac{\hat{O}\Psi_T}{\Psi_T}$ evaluated for walker j at time step k. Now we assume two perturbations of the form $\alpha\hat{O}_A$ and $\beta\hat{O}_B$, and following Ref. 6 we obtain growth and direct estimators of the response function $\chi_{AB}=\frac{\partial\langle\hat{O}_A\rangle}{\partial\beta}=\frac{\partial\langle\hat{O}_B\rangle}{\partial\alpha}$ from the second derivative of the growth and direct estimators of the energy

$$\chi_{AB}^{GR}(i) = -t[\overline{X_i^A X_i^B} - \overline{X_i^A}\cdot\overline{X_i^B}], \tag{3}$$

$$\chi_{AB}^{E}(i) = -t[\overline{X_i^A O_i^B} - \overline{X_i^A}\cdot\overline{O_i^B} + \overline{O_i^A X_i^B} - \overline{O_i^A}\cdot\overline{X_i^B}] + t^2[\overline{(E_i^L - \overline{E_i^L})(X_i^A - \overline{X_i^A})(X_i^B - \overline{X_i^B})}]. \tag{4}$$

Any number of operators $\hat{O}^A$ and $\hat{O}^B$ can be sampled in parallel within a single DMC run. At this point it is important to note that while we let the Hamiltonian vary with α and β the variation in the quantum system is constrained to a Hilbert space with the nodes kept frozen at their $\alpha=\beta=0$ position even for nonzero values of α and β because the method is based on performing a single fixed-node DMC calculation at $\alpha=\beta=0$. In the case of evaluating expectation values the result is equivalent to using the fixed-node approximation.[6]

From now on we use the Fourier components of the density $\sin \boldsymbol{kx}$ and $\cos \boldsymbol{kx}$. Note also that, as in the case of the first derivative discussed in Ref. 6, the growth estimator at i is already an averaged quantity. This property makes it an attractive choice for a DMC calculation. Equation (4) is not only a more complicated formula than Eq. (3), it also has to be summed at each time step i. If we wish to sample many components of χ at the same time, a large array with a size quadratic in the number of components of χ in Eq. (4) has to be generated and dealt with at each time step. By contrast, Eq. (3) only has to be built at whatever time step one wishes to calculate χ. This means that at each time step one only has to maintain the $X_i^{A/B}$, which is less memory intensive and much faster to compute. Hence we shall only use the growth estimator Eq. (3).

B. Computational implementation

The growth estimator has the advantage that for each time step and walker we only need to deal with simple sampling of N_k variables for the components of the density. The entire density-response function, including off-diagonal elements, can then be calculated as a correlation function[9] of these variables at the end of the run saving computer time and memory. As in HFS, we find that noise rises as the sampling progresses, thus limiting the statistical error of the final result even if the sampling is continued indefinitely. So to reduce statistical noise, we increase the number of walkers instead. This has the additional advantage of reducing any population bias. We converged this by looking at population sizes of 200, 1000, 5000, and 50 000 walkers. We used the latter for the main results shown here (at $N_{el}=114$ electrons). Looking at different time steps, we found that too large a time step shows up as a leveling off of χ at a finite value at larger k instead of showing the correct $1/k^2$ behavior. Interestingly, even at $\Delta t=0.1$ the calculated χ remained unbiased up to and well beyond $k=5k_F$. A large time step is desirable as equilibration will be faster. Here we use $\Delta t=0.01$. To monitor equilibration we artificially extract a value $\tilde{\chi}_i$ that when summed over all time steps $1,\ldots,N$ gives the growth estimator $\chi(N)$ at time step N of sampling: from

$$\frac{1}{N-1}\sum_i^{N-1}\tilde{\chi}(i) = \chi(N-1) \tag{5}$$

and

$$\frac{1}{N}\sum_i^{N}\tilde{\chi}(i) = \chi(N) \tag{6}$$

it follows that

$$\tilde{\chi}(N) = N\chi_N - (N-1)\chi(N-1). \tag{7}$$

Following, e.g., three typical k's as the sampling progresses we found that $\tilde{\chi}$ converges exponentially. A quick run using few walkers in a smaller system can then be used to roughly estimate the convergence time which one then uses in an actual run. Convergence can be improved by setting up the sampling such that one ignores the implied $\tilde{\chi}$ during equilibration. In order to do that it is not necessary to actually reverse engineer these $\tilde{\chi}$ for each element of the density response function. Once one has decided on an equilibration time, N_{eq} the desired result is

$$\frac{1}{N-N_{eq}}\sum_{i=N_{eq}+1}^{N}\tilde{\chi}(i) = \frac{1}{N-N_{eq}}[N\chi(N) - N_{eq}\chi(N_{eq})]. \tag{8}$$

It is thus sufficient to perform the costly sampling of the full growth estimator only twice during the run, once after equilibration, and once at the end of the run. Doing so, efficiently removes much of a $1/N$-like term without incurring much extra computation. We found that equilibration was essentially independent of δt and seemed to depend only weakly on the population size. We note that while in this paper we only calculate the diagonal terms of χ, sampling the full density-response function, including all the off-diagonal terms, is not more difficult: all that is needed is the evaluation of the correlation function of X_ks at different k and k'.

III. RESULTS

A. System

In order to demonstrate our method we calculated the diagonal terms of the static density response function of an unpolarized free electron gas for electron-density parameter $r_s=2$, 5, and 10 and corresponding density n_0. We set up the

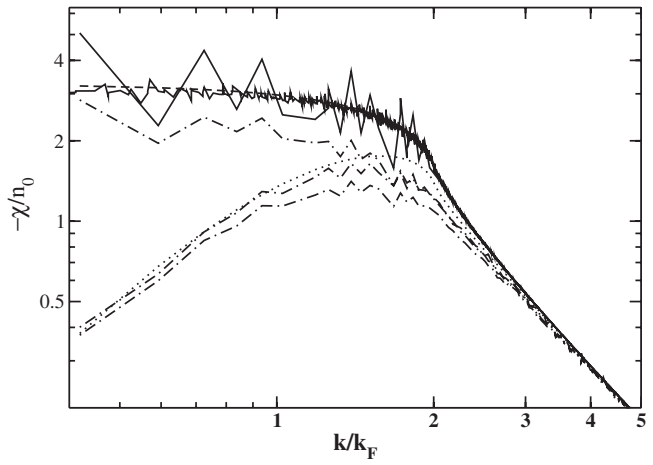

FIG. 1. The dashed line shows the density response function χ_0 of an infinitely large unpolarized noninteracting homogeneous electron gas (Lindhard function) at $r_s=2$. The black lines close to the Lindhard function show the exact finite-size Lindhard function χ_0^{fs} with 114 and 4218 electrons, the latter following the Lindhard function closer. The dotted line shows the RPA response function χ_{RPA}, and the three remaining dot-dashed lines show (from top to bottom) the frozen-node Lindhard function χ_0^{fn} at 114 electrons, the corresponding frozen-node density response of an interacting system χ^{fn}, and the frozen-node RPA $\chi_{\mathrm{RPA}}^{\mathrm{fn}}$. The "wiggles" are not noise [see Fig. 2 and the text for details] as they correspond to the shell structure seen in the exact noninteracting finite size χ_0^{fs}.

DMC calculation using 114 electrons in a simple-cubic super cell. We also looked at *fcc* unit cells and smaller systems with 66 electrons, however, we found no significant difference. In all, we calculated the density response at all 119 independent k vectors between $k=0$ and $k=5k_F$. Our DMC calculations employed trial wave functions Ψ_T of the Slater-Jastrow type with a standard correlation term. Prior to the DMC run Ψ_T was optimized in a variance minimization run. We used the CASINO (Ref. 10) code for all our computations.

B. Density-response function

In general, the response function is given by

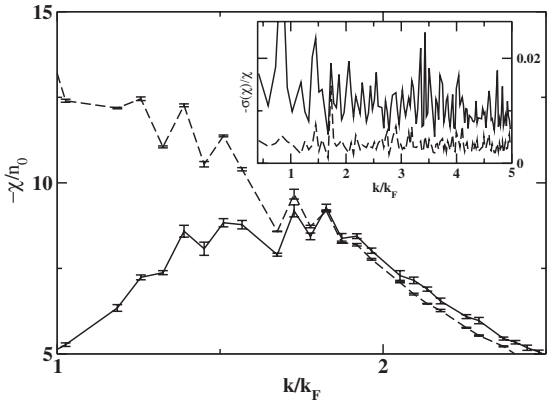

FIG. 2. χ^{fn} (solid line) and χ_0^{fn} (dashed line) at $r_s=5$ including error bars calculated as described in the text. The inset shows relative errors. Note that these seem to be independent of k. The results for $r_s=2$ and 10 are similar.

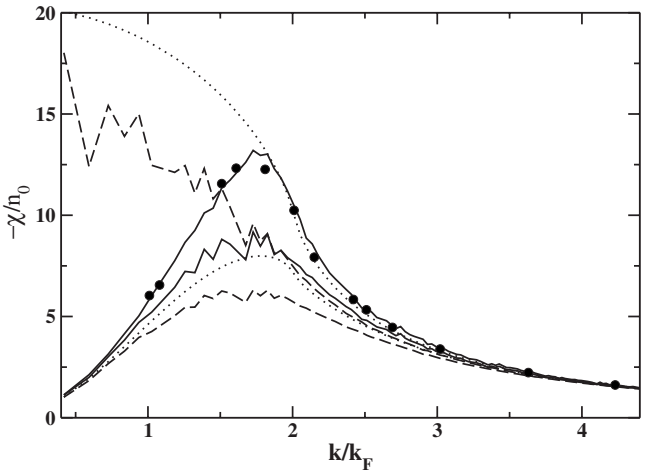

FIG. 3. The density response at $r_s=5$ for an unpolarized 114 particle homogeneous electron gas. The dotted lines show the Lindhard function χ_0 (top) and χ_{RPA} (bottom). The dashed lines are χ_0^{fn} (top) and $\chi_{\mathrm{RPA}}^{\mathrm{fn}}$ (bottom). Finally, the solid lines show the fixed node χ^{fn} (bottom) and extrapolated interacting χ. The dots correspond to the results in Ref. 2. Our data reaches to smaller k values as our system is larger (114 vs up to 66 electrons).

$$\chi_{AB} = \sum_{i=1}^{\infty} 2\Re \frac{\langle 0|\hat{O}_A|i\rangle\langle i|\hat{O}_B|0\rangle}{E_0 - E_i}, \tag{9}$$

where the sum runs over all excited states of the many-electron system. fn DMC yields the ground-state energy for nodes given by the trial wave function. Therefore the second derivative yields the fixed-node response χ^{fn} of a system for which the nodes are the same for all perturbing potentials. Since in the case of a fixed-node system the sum entering Eq. (9) runs over a set of fixed-node excited states that differ from the actual excited states of the many-electron system, the fixed-node and nonfixed-node noninteracting density-response function differ considerably (Fig. 1). Another inter-

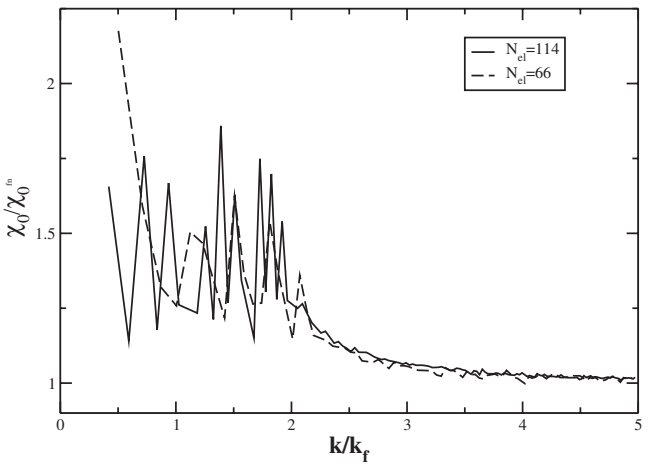

FIG. 4. The ratio $\frac{\chi_0}{\chi_0^{\mathrm{fn}}}$ at $r_s=5$ for $N_{el}=66$ and $N_{el}=114$ electrons. Except for the omnipresent DMC noise [see Fig. 2] this graph is independent of the value of r_s due to scaling. Note the pronounced shell structure for $k<2k_f$.

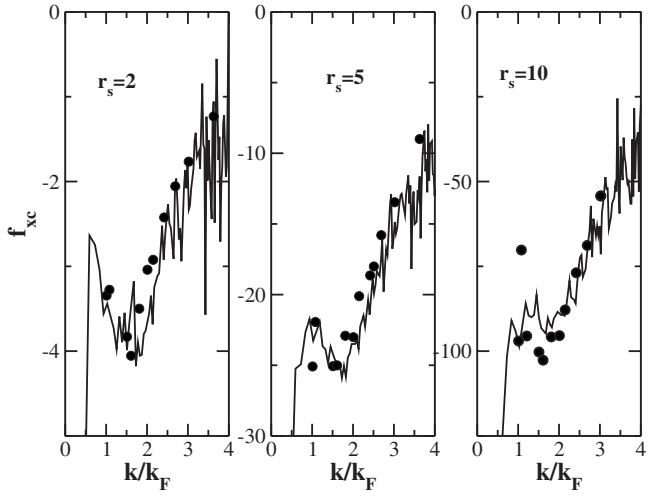

FIG. 5. $f_{\mathrm{xc}}^{\mathrm{fn}}$ at $r_s=2,5,10$. The value at $k=0.4189k_F$ clearly is an outlier. Interestingly, there is a slight dip in $f_{\mathrm{xc}}^{\mathrm{fn}}$ for $k/k_F<2$ as demonstrated in Ref. 12. The dots correspond to the data in Ref. 2.

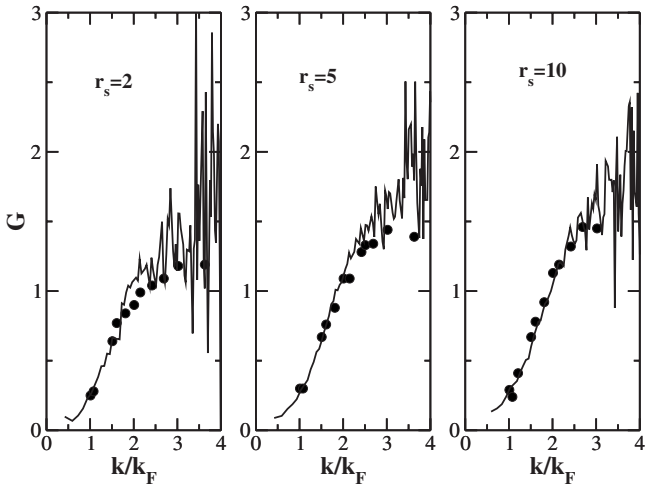

FIG. 6. As Fig. 5 but showing the local field factor.

esting observation is the shell structure exhibited by all finite-size (fs) results. In order to visualize both the fixed-node error and the finite-size effects, we have plotted in Fig. 1 the following calculations: the static density-response function of (i) an infinitely large noninteracting free electron gas, the well-known Lindhard function[11] χ_0 (dashed line), (ii) χ_0^{fs} of a noninteracting system of 114 and 4218 electrons (solid lines), (iii) an infinitely large interacting free electron gas in the random-phase approximation (RPA), χ_{RPA} (dotted line), (iv) a finite system of 114 noninteracting electrons within the frozen-node approximation giving χ_0^{fn} (top dot-dashed line), (v) a finite system of 114 interacting electrons within our frozen-node DMC scheme (middle dot-dashed line), and (vi) a finite system of 114 interacting electrons in the fn RPA $\chi_{\mathrm{RPA}}^{\mathrm{fn}}$ (dot-dashed line at the bottom, see below for details). We see that the finite-size shell structure is not negligible even for a system of 4218 electrons. Nevertheless, the exact noninteracting density-response function nicely reproduces the well-known Lindhard function especially for $k/kf>2$.

To support the notion that the "wiggles" in Fig. 1 are the result of a shell structure and not statistical noise we have also estimated the latter in Fig. 2: the DMC calculations yield data for all k vectors and each data point in our figures is, in fact, an average over between six and 64 underlying k vectors of the same length. This multiplicity allows us to estimate the statistical error. For each value of r_s we also performed two independent DMC runs and the differences between these (not shown) are consistent with our estimate of the error bars.

C. Discussion

Since the fn Lindhard function χ_0^{fn} (top dashed line in Fig. 3) is smaller than the real Lindhard function χ_0 (dotted line at the top of Fig. 3) the fn interacting χ^{fn} is also too small (lower solid line in Fig. 3 compared to the dots showing the relevant data of Ref. 2). However, assuming that the effect of the fixed-node nature of the calculation is the same for the interacting and noninteracting case, we should still be able to extract meaningful correlation data and reverse the effects of the fn approximation.[8] Let us start with the definition for the exchange correlation (xc) kernel f_{xc} and the local field factor G

$$
\begin{aligned}
-f_{\mathrm{xc}}(k) &= v_C(k)G(k) \\
&= \frac{1}{\chi(k)} - \frac{1}{\chi_{\mathrm{RPA}}(k)} \\
&= \frac{1}{\chi(k)} - \frac{1}{\chi_0(k)} + v_C(k),
\end{aligned}
\tag{10}
$$

where $v_C(k)=\frac{4\pi}{k^2}$. In practice, we do not have access to $\chi(k)$ but only to its finite-size equivalent in the fixed-node approximation. Moroni and co-workers,[2] who include the nodal variation at a Kohn-Sham level argue that while the density response contains finite-size effects, f_{xc} is less afflicted by these. Hence, they extract f_{xc} and add that back on to the nonfixed-node infinite-cell Lindhard function to correct for finite-size effects, thus eliminating the shell structure. There is no reason to expect the nodal variation in the KS nodes to correctly describe the nodal variation in the fully interacting system with respect to χ: the KS nodes and the true many-body nodes are unrelated. Furthermore, different DMC systems at different numbers of electrons N_{el} also correspond to distinct nodes but the data for f_{xc} (e.g., Ref. 2 or Fig. 8) for different values of N_{el} is mutually compatible. Finally, the effect of the nodal variation on χ_0 seems universal, i.e., independent of N except for shell effects (see Fig. 4). It therefore seems reasonable to assume that f_{xc} is independent of nodal effects and can thus be used to correct for wrong or absent nodal variation. Hence, by using the frozen-node quantities in Eq. (10), implicitly defining a frozen-node $\chi_{\mathrm{RPA}}^{\mathrm{fn}}$, we can derive a fn $f_{\mathrm{xc}}^{\mathrm{fn}}$ and G^{fn} (Figs. 5 and 6). These are remarkably similar to the data in Ref. 2. In fact, $f_{\mathrm{xc}}^{\mathrm{fn}}$ even has a slight dip as suggested in Ref. 12 which however is not really visible in Ref. 2. This is encouraging and indeed we can use our data for G^{fn} in conjunction with the real χ_{RPA} in Eq. (10) to estimate the non-fn interacting χ. The result can

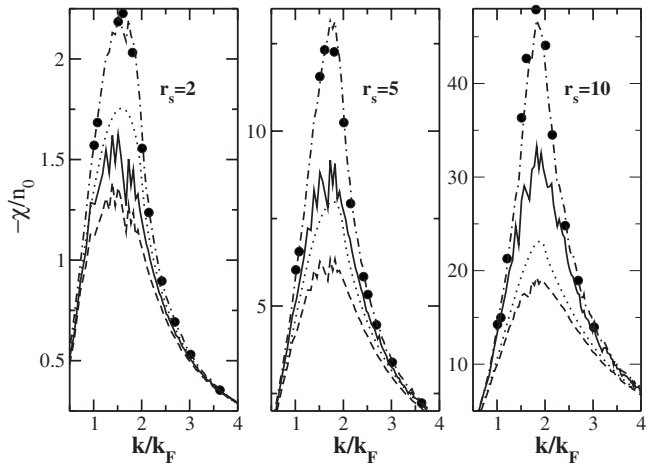

FIG. 7. RPA (dotted), fn RPA (dashed), fn DMC (solid), and extrapolated (dot-dashed) density response function calculated using a 114 particle homogeneous electron gas at $r_s=2$, 5, and 10. The dots correspond to the results in Ref. 2. Note that for $r_s=2$ the uncorrected DMC data is lower still than standard RPA.

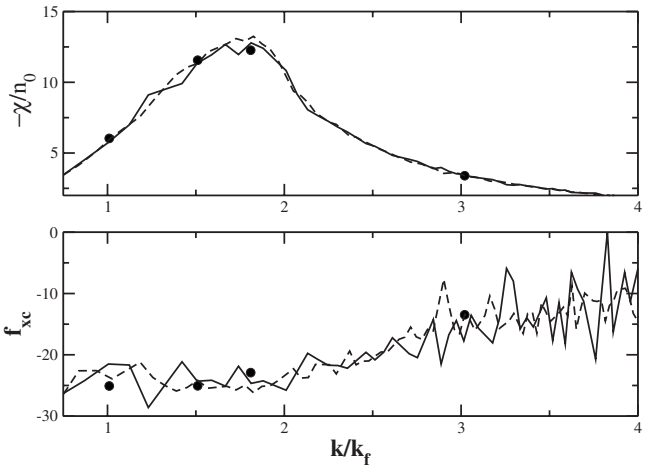

FIG. 8. A comparison of our results for f_{xc} at $r_s=5$ and the finite size corrected χ with the data in Ref. 2 where comparison is possible, i.e., at $N_{el}=66$ electrons. All our other data uses a larger simulation cell with 114 electrons and more configurations in the DMC run. The solid dots are the four data points for $N_{el}=66$ electrons of Ref. 2 and the solid line corresponds to our data (just under 100 data points in the shown region). The dashed line shows our data for the $N_{el}=114$ electron system. As suggested in Ref. 2 there is no significant difference between $N_{el}=66$ and $N_{el}=114$. Note that for $N=66$ we use fewer walkers than for our main results at $N=114$.

be seen in Fig. 3: all the fn quantities are too small compared to their non-fn counterparts. However our extrapolated data (solid line at the top) is very close the extrapolated data of Ref. 2 (dots).

For completeness sake Fig. 7 shows details of the extrapolated χ at $r_s=2$, 5, and 10. Also, in Fig. 8 we show a direct comparison between our results and Ref. 2 where it is possible, i.e., at $N_{el}=66$ electrons in addition to our results for $N_{el}=114$ electrons confirming that all our data is compatible with Ref. 2. Except for noise there is no significant difference between data at different N_{el}, corroborating the assumption that f_{xc} is independent of finite-size effects.

In general, our results nicely follow the data in Ref. 2, who take into account the change in the nodes at a Kohn-Sham level, whereas our calculations do not take into account any nodal effect on xc quantities. The fact that the methods yield consistent results for f_{xc} suggest that assuming f_{xc} to be free from nodal effects is justified and that in either case the resulting data is an accurate description of systems with the full interacting nodal variation.

IV. CONCLUDING REMARKS

We have generalized Ref. 6 to the second derivative of the energy. This yields a novel method and an efficient algorithm to calculate the static response function within DMC. Our algorithm permits the computation of a large number of diagonal and off-diagonal terms in a single DMC run without the need for numerical derivatives or reoptimization. Noise can be efficiently controlled by increasing the number of DMC walkers and we have found that we can use large DMC time steps without introducing a bias, potentially speeding up calculations greatly. The wave function nodes have a strong effect on χ, particularly for $k<3k_F$ and generalizing the RPA analysis using χ_0^{fn} yields a frozen-node $\chi_{\mathrm{RPA}}^{\mathrm{fn}}$. Using this to extract the xc contribution of χ we find that our method's results are broadly in line with previous DMC calculations[2] which, however, are much more cumbersome, yield potentially fewer data points, and are effectively limited to diagonal terms only.

ACKNOWLEDGMENTS

This work has been supported by the Basque Unibertsitate eta Ikerketa Saila and the Spanish Ministerio de Ciencia e Innovacion (Grants No. FIS2006-01343 and No. CSD2006-53). Computing facilities were provided by the Donostia International Physics Center (DIPC) and the SGI/IZO-SGIker UPV/EHU (supported by the National Program for the Promotion of Human Resources within the National Plan of Scientific Research, Development and Innovation-Fondo Social Europeo, MCyT and the Basque Government).

*Present address: Faculty of Physics, University of Vienna, and Center for Computational Materials Science, Sensengasse 8/12, A-1090 Vienna, Austria.

[1] W. M. C. Foulkes, L. Mitas, R. J. Needs, and G. Rajagopal, Rev. Mod. Phys. **73**, 33 (2001).
[2] S. Moroni, D. M. Ceperley, and G. Senatore, Phys. Rev. Lett. **75**, 689 (1995).
[3] C. Bowen, G. Sugiyama, and B. J. Alder, Phys. Rev. B **50**, 14838 (1994).
[4] A. L. Fetter and J. D. Walecka, *Quantum Theory of Many-Particle Systems* (McGraw-Hill, New York, 1971).
[5] E. Runge and E. K. U. Gross, Phys. Rev. Lett. **52**, 997 (1984).
[6] R. Gaudoin and J. M. Pitarke, Phys. Rev. Lett. **99**, 126406 (2007).
[7] R. P. Feynman, Phys. Rev. **56**, 340 (1939).
[8] Note that the analysis leading to RPA (e.g. Ref. 4) does not mention nodes and thus should apply equally to the fn system.
[9] Another method [J. Vrbik and S. M. Rothstein, J. Chem. Phys. **96**, 2071 (1992)] to calculate vibrational frequencies yields similar looking formulae. However, that method cannot be used for the exact fn sampling of general operators, only gives the fn response with respect to a parameter such as the distance between atoms, and applies specifically to DMC with fully retained weights.
[10] R. J. Needs, M. D. Towler, N. D. Drummond, and P. López Ríos, J. Phys.: Condens. Matter **22**, 023201 (2010).
[11] D. Pines and P Noziers, *The Theory of Quantum Liquids* (Benjamin, New York, 1966).
[12] B. Farid, V. Heine, G. E. Engel, and I. J. Robertson, Phys. Rev. B **48**, 11602 (1993).